Dual Fluidized Bed Gasification Configurations for Carbon Recovery from Biomass

energy&fuels

pubs.acs.org/EF

Article

Dual Fluidized Bed Gasification Configurations for Carbon Recovery from Biomass

Sébastien Pissot,* Teresa Berdugo Vilches, Henrik Thunman, and Martin Seemann

Cite This: *Energy Fuels* 2020, 34, 16187−16200

Read Online

ACCESS | Metrics & More | Article Recommendations

ABSTRACT: Techniques that produce chemicals and fuels from sustainable carbon sources will have to maximize the carbon recovery to support circularity. In dual fluidized bed (DFB) gasification, to facilitate carbon recovery, the CO_2 from the flue gas can be concentrated using pure oxygen as an oxidant. The heat required by the process can also be provided electrically or by oxidizing an oxygen-carrying bed material, rather than combusting part of the char, thereby concentrating all of the carbon in the syngas. In this work, the three configurations of oxyfuel, electrical, and chemical-looping gasification (CLG) are compared to each other, as well as to the standard or "air" configuration, which corresponds to the combustion of char with air and the separation of CO_2 from both the flue gas and syngas. The configurations are compared based on their carbon distributions and energy demands for CO_2 separation. We show that the air and oxyfuel configurations lead to similar carbon distributions, whereas the CLG configuration gives the lowest carbon recovery in the form of an end product. The oxyfuel and CLG configurations show the lowest energy demands for CO_2 separation, while the air configuration exhibits the highest. The electrical configuration has the lowest potential to benefit from heat integration to cover this energy demand. An investigation into the optimal gasification temperature for the air and oxyfuel configurations shows that there is no driver for operation at high temperatures.

1. INTRODUCTION

One of the main challenges faced by humanity in the 21st century is the need to produce goods in a sustainable manner to maintain a high quality of life across the globe. However, most consumer goods are based on carbon, the current utilization of which is far from sustainable. Products such as paper and cardboards are sourced from renewable biomass and are recycled at relatively high rates. Thus, 38% of the input for paper production is waste paper.[1] Products such as plastics, fibers, and resins are based on fossil fuels and, in most cases, their carbon content is lost, either in landfills or into the atmosphere when they are incinerated. The depletion of fossil resources and the accumulation of carbon in the form of CO_2 in the atmosphere, resulting in global warming,[2] must be addressed by developing a new carbon system, whereby carbon is extracted from sustainable sources such as biomass or biogenic waste, while simultaneously contributing to neutral or even negative emissions of CO_2. This would contribute to minimizing global warming. Ideally, such a system would rely almost entirely on waste products to generate new carbon-based materials, despite the inevitable losses, which would be compensated for by harvesting biomass.[3] However, this will require carbon-extracting technologies that enable the production of carbon-based materials of virgin quality (i.e., of a quality similar to that of the original). For this reason, thermochemical processes that convert waste into building blocks for new materials are likely to be a cornerstone of the future carbon system.

Thermochemical processes break down the solid carbonaceous matrix of biomass and organic waste materials into a variety of liquid and gaseous compounds. In these processes, CO_2 is produced both directly (through degradation of the material and its reaction with the surrounding gas environment) and indirectly (as a byproduct of the generation of heat required by the thermochemical processes). The produced CO_2 can be reacted to increase the amount of carbon-based material produced from the source material or it can be sequestered or emitted into the atmosphere. The latter option is undesirable but may be acceptable if it results in low levels of emissions. Nonetheless, and despite the attractiveness of producing materials from CO_2, neutral and negative emissions achieved via carbon capture and storage (CCS) will likely be needed to limit the impact of global warming.[4]

Many thermochemical processes have been investigated, both academically and industrially. For an overview of the state of thermochemical conversion processes, with a focus on pyrolysis and gasification, the readers are referred to the reviews of Sikarwar et al. on biomass gasification,[5] Uddin et al. on biomass pyrolysis,[6] and of Al-Salem et al. on recycling of plastic solid waste.[7] Among the existing thermochemical processes, dual fluidized bed (DFB) gasification presents a number of attractive features, including its flexibility in terms of fuel input, high heat- and mass-transfer rates, homogeneous temperature profile, and the production of raw gas not diluted with nitrogen, without the need for producing pure oxygen. DFB gasifiers have been tested

Received: August 17, 2020
Revised: October 26, 2020
Published: November 11, 2020

at the industrial scale with biomass[8−10] and at the semi-industrial[3,11,12] and pilot[13,14] scales with plastic waste. As shown in Figure 1, a DFB gasifier consists of two interconnected

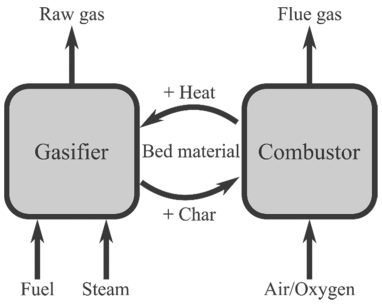

Figure 1. Schematic of a dual fluidized bed gasifier.

reactors: a gasifier, in which the fuel reacts with steam to form a raw gas, and a combustor, where part of the char from the fuel is burnt to produce the heat required for the gasification reactions, with the char and heat being transported by the bed material that circulates between the two reactors. Fluidized beds are suited to the extraction of carbon from biomass and waste, as they are flexible in terms of input fuel and require little or no preparation of the fuel. This is an important aspect, given that postconsumer waste is expected to be highly heterogeneous and that the biomass from which carbon will be extracted will likely be low-value biomass such as recovered wood. This will avoid competition with other usages of the biomass and land areas. The use of fluidized beds also facilitates the introduction of additives that limit emissions, e.g., limestone for desulfation and the capture of chlorine. These additives can also act as catalysts to optimize the output of the gasifier.

In a DFB gasifier, the segregation of the heat production to another reactor and the possibility to produce the heat in a variety of ways, apart from the combustion of char, mean that the process can be operated in various configurations. In the standard DFB gasification configuration, complete recovery of the carbon with sequestration of the CO_2 entails the separation of CO_2 from the syngas exiting the gasifier and the flue gas exiting the combustor. In the latter, the CO_2 is expected to be rather diluted, which incurs high costs for separation. To address this issue, two strategies can be employed: (1) enhancing the separation of CO_2 from the flue gas by increasing its concentration or (2) avoiding the need for separation by providing heat without oxidation of carbon in the combustor, thereby recovering all of the carbon in the syngas as either product or CO_2. The first strategy involves replacement of part or all of the air in the combustor with pure oxygen, which is referred to as the "oxyfuel configuration" in this work. For the second strategy, two configurations, referred to as the "carbon-free heat production configurations", are investigated. The heat can be provided by electric heating, for instance by installing electrical coils in the bed material loop before the combustor, which is retained for its role as a regenerator of the bed material. This configuration is referred to as the "electrical configuration". Alternatively, the heat can be produced by taking advantage of the exothermic reactions of certain metal-based bed materials with the oxygen in the air, in a configuration referred to as "chemical-looping gasification" (CLG).[15]

The DFB gasification technology has been extensively investigated, albeit mainly with respect to optimizing the conversion to tar-free syngas in the gasifier. Rarely has the DFB gasifier been placed in the context of a plant producing a specific (generally hydrocarbon) end product. Furthermore, the recovery of carbon from the CO_2 produced by the DFB gasifier and the downstream upgrading and synthesis steps have not been in focus in the literature. In the future, two factors will be crucial in evaluating DFB gasification plants: (1) their carbon recovery potential, i.e., the fraction of carbon from the carbon source that is recovered as an end product and CO_2, and (2) their potential for neutral or negative emissions through the sequestration of CO_2. Therefore, the aim of the present work is to investigate the potential for carbon recovery of the DFB gasification technology, by comparing its possible configurations. This comparison is made on the basis of the distributions of the carbon that they produce (Figure 2), i.e., the distribution of carbon among the end product, the CO_2 separated from the syngas, and the CO_2 in the flue gas, and on the basis of their carbon recovery prospects. The challenge posed by the CO_2 separation step is assessed by evaluating the reboiler heat duty and the CO_2 concentrations in the relevant streams. The optimal operation of the DFB gasification configurations is discussed, in particular by investigating the effects of the temperature of the gasifier on the carbon distribution and the CO_2 separation process. This paper focuses

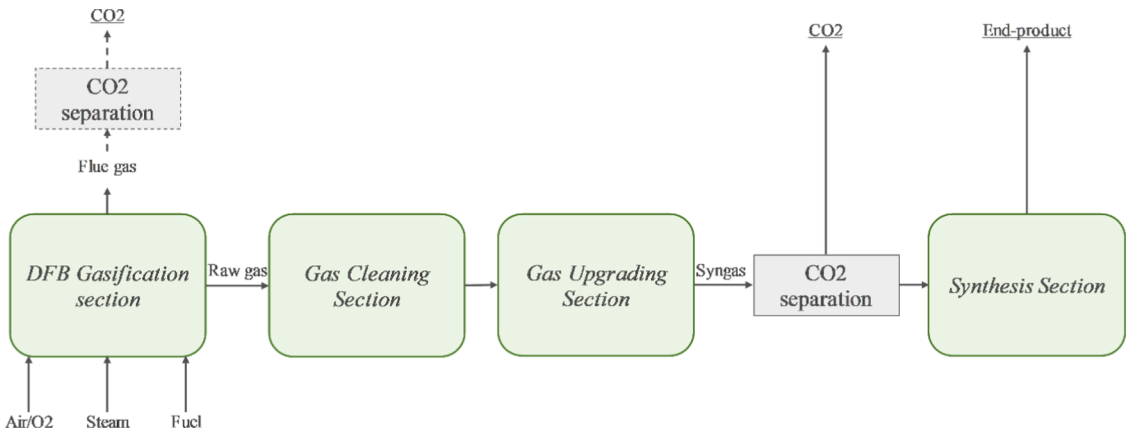

Figure 2. Schematic of a DFB gasification plant, whereby raw gas is upgraded and synthesized to a specific end product, and CO_2 is separated. The dashed box for the separation of CO_2 from the flue gas indicates that this is an optional step, as the flue gas can be released directly into the atmosphere (after some cleaning steps).

https://dx.doi.org/10.1021/acs.energyfuels.0c02781
Energy Fuels 2020, 34, 16187−16200

on biomass as a carbon source since most of the DFB gasification literature focuses on biomass. Moreover, only biomass has been converted in large-scale DFB gasification plants.

2. DESCRIPTIONS OF THE DFB GASIFICATION CONFIGURATIONS

This section discusses the various configurations of the DFB gasification technology and their potentials for carbon recovery. First, the DFB gasification based on oxidation of part of the char in the combustor, referred to in this paper as the "air configuration" or "regular DFB gasification", is described. This configuration is used as the reference from which the other configurations are derived, as it is the most investigated among the DFB gasification configurations and the only one that has been tested at the industrial scale. Possibilities to steer the carbon distribution and recovery are discussed. Note that these possibilities are also relevant to the optimization of the carbon distributions of the other configurations. In the following section, the "carbon distribution of the raw gas" refers to the distribution of carbon in the various species that constitute the raw gas. The overall carbon distribution represents the distribution of carbon between the CO_2 in the flue gas, the CO_2 separated from the syngas prior to synthesis, and the carbon in the end product, i.e., that produced by the synthesis step (Figure 2). The overall carbon distribution is referred to simply as the "carbon distribution" unless another type of carbon distribution is mentioned.

2.1. Regular DFB Gasification. As described in Section 1, the regular DFB gasification relies on the combustion of part of the fuel that leaves the gasifier to cover the heat demand of the DFB process. The heat demand can also be met by combustion of part of the product gas from the gasification or the tar, along with its sorbent if tar cleaning is performed with a scrubbing medium.

If the goal of the gasification plant is to produce a chemical species as the end product, then the synthesis of that species will require a syngas with a specific H_2/CO ratio. Therefore, in the present work, it is assumed that the raw gas from the gasifier will be reformed, thereby converting all of the hydrocarbons to H_2 and CO, and that the H_2/CO ratio will be adjusted via the water−gas shift (WGS) reaction. Note that while this approach is chosen for all of the DFB configurations to ensure comparability, it does not necessarily reflect the technology choices that will be most beneficial economically.

A consequence of the reforming and WGS of the raw gas is that tuning the carbon distribution of the raw gas via reforming and cracking reactions of hydrocarbons in the gasifier will not affect the overall carbon distribution since the operation of the reforming step will be adjusted to produce a syngas containing only H_2, CO, and CO_2. Therefore, affecting the reforming and cracking reactions in the gasifier only displaces the reactions from the reformer to the gasifier. Thus, the only way to adjust the overall carbon distribution is to tailor the heat demand of the DFB gasification process and change the way in which the heat demand is covered, which will alter the distribution of carbon between the flue gas and raw gas. The heat demand can be decreased by operating at a lower temperature, preheating the air and steam, preheating and drying the fuel, or decreasing the heat losses from the system. Note that the reactions in the gasifier also influence the heat demand, although they are unlikely to be used as a means to adjust the heat demand. The gasification, reforming, and cracking reactions increase the heat demand, whereas the WGS reaction decreases it.

Even though tuning the carbon distribution of the raw gas is not a viable strategy for adjusting the overall carbon distribution, enhancing the reactions that reduce the amount of tar and shift their composition toward less-troublesome species is desirable. With increasing temperature of operation, the tar increasingly undergoes reforming and cracking reactions potentially followed by polymerization reactions at higher temperatures, thereby creating polyaromatic hydrocarbons and, ultimately, soot.[16] The choice of the operating temperature to minimize the deleterious impact of tar on the operation will, therefore, be a balance between the amount of tar and the tar composition. The reactions that involve tar and precursors thereof can be affected by the use of catalytic materials[17−19] or by the interaction of the bed material with the fuel ash, leading to the development of catalytic activity.[20−30] Nevertheless, the materials that catalyze the tar reactions will also likely affect the reforming and cracking reactions of light hydrocarbons, and they can also catalyze the WGS reaction. As noted in the previous paragraph, this will result in an increase in the heat demand of the process.

2.2. Concentrating the CO_2 in the Combustor: Oxy-combustion-Based DFB Gasification. The removal of CO_2 from the flue gas is challenging due to its relatively low concentration, which is expected to be around 15%, comparable to the concentrations found in the flue gases of combustors. The separation step can be facilitated or even avoided by replacing part or all of the air with pure oxygen. The remaining oxygen in the flue gas can be removed in a postoxidation step, and the gas can be made ready for compression and storage following some cleaning steps. Typically, a large fraction of the flue gases must be recycled to control the temperature in oxyfuel combustion since combustion in pure oxygen leads to very high adiabatic flame temperatures.[31] This also enables one to control the bed circulation independently of the oxygen requirement. The state-of-the-art technique for the production of pure oxygen is the cryogenic separation of oxygen from air in an air separation unit (ASU). The typical electrical energy requirement of such a process is 0.7 MJ/kg O_2 (200 kWh/tonne).[32]

Another way to concentrate CO_2 in the flue gas of the combustor is to use a bed material capable of adsorbing CO_2 in the gasifier and releasing it in the combustor, in a process often referred to as "sorption-enhanced reforming".[33] This process has been investigated for its potential to produce a syngas particularly rich in H_2, and the use of oxyfuel combustion in the combustor to further increase the CO_2 concentration in the flue gas has been investigated.[34] The sorption-enhanced reforming configuration is not treated in this work.

2.3. Carbon-Free Heat Production Configurations. *2.3.1. Electrical DFB Gasification.* The heat demand of the DFB gasification process can be covered partly or entirely using electrically heated tube banks immersed in the bed material, ideally placed in a fluidized section before the combustor, to avoid erosion.[3] Although direct heating of the gasifier is possible, retaining the combustor is advantageous. It offers the possibility to deal with sidestreams and waste streams that may be too challenging to treat otherwise, such as tar and raw gas fly ash, which contains carbon that has been elutriated and cannot be converted in the gasifier. This enables the recovery of the carbon from the tar and raw gas fly ash as CO_2 in the flue gas; however, the amount of carbon thus recoverable may be too small to justify the cost of a CO_2 separation column. Finally, retaining the combustor also serves as a means to regenerate the bed material, for instance, from coking.

https://dx.doi.org/10.1021/acs.energyfuels.0c02781
Energy Fuels 2020, 34, 16187−16200

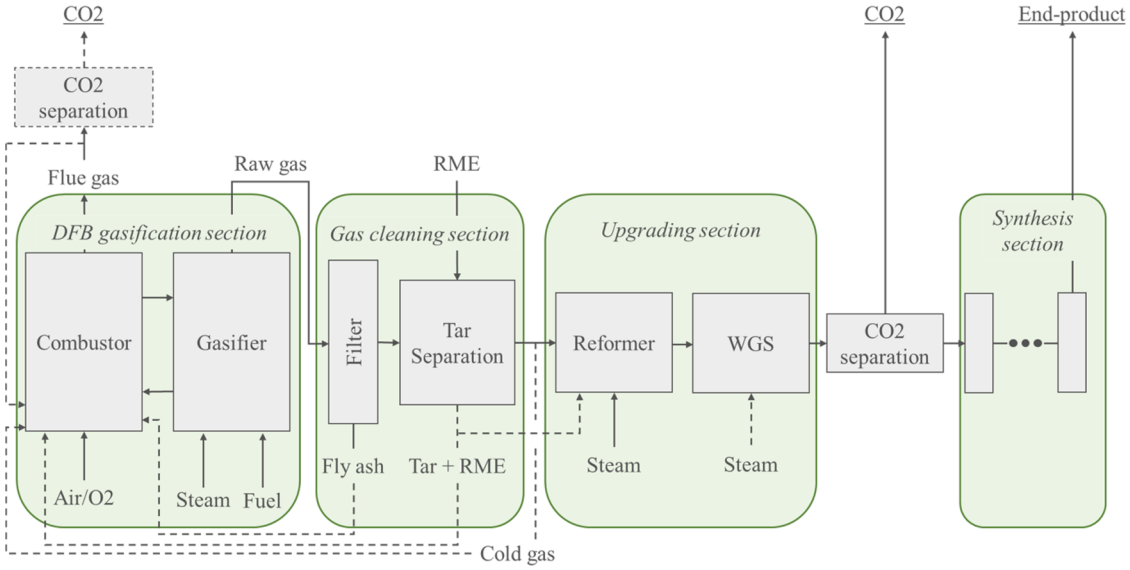

Figure 3. Layout of the DFB gasification plant considered in this work. The dashed arrows represent optional pathways. The dashed box for CO_2 separation signifies that this separation step is optional. The underlined text items indicate the final outputs from the plant.

2.3.2. Chemical-Looping Gasification. The CLG configuration of the DFB has attracted much interest for its potential to convert fully a solid fuel into syngas, thereby allowing the recovery of all of the carbon in a single, undiluted stream. The CLG concept is based on the use of oxygen carriers as bed materials in a DFB gasification system.[15,35] These oxygen carriers are materials, usually metals, that react with the oxygen from the air at high temperatures, releasing a large amount of heat, comparable to that produced by the combustion of char (per molecules of O_2 reacted). In the gasifier, the oxygen that is taken up is released by reacting with the gas. Some oxygen carriers can even release their oxygen to the gas phase, where it can react with the gas or char, thereby contributing to the gasification process.[36] Note that, in the literature on CLG, the reactor in which oxidation of the bed occurs is referred to as the "air reactor" rather than the combustor, and the reactor in which gasification occurs is referred to as the "fuel reactor". This nomenclature will be used in this work when discussing CLG. Nonetheless, the units are to be understood as conceptually similar, despite the different nomenclatures.

Ideally, the release of oxygen would increase rather than decrease the quality of the gas, for instance, by oxidizing troublesome species such as tar, to form CO and H_2. However, the oxidation would likely continue to produce CO_2 and H_2O. Furthermore, the concentrations of undesired species are much lower than those of the syngas and light hydrocarbons. In particular, the concentrations of H_2 and CO are high, and these are small and reactive molecules that are much more likely than larger molecules to react with the oxygen on the surface of the oxygen carrier. Consequently, there is a risk that using oxygen carriers will lead to a transfer of carbon from CO and light hydrocarbons to CO_2. Despite this, there are still possibilities to increase the quality of the gas, in terms of increasing cracking and reforming of tar, by mixing the oxygen carrier with a catalytic bed material without oxygen-carrying capability or by operating the air reactor at lower excess air ratios to increase the amount of reduced oxygen carrier leaving the air reactor, as suggested by Dieringer et al.[37] Nevertheless, the downstream upgrading and synthesis steps need to be accounted for in determining how this influences the overall carbon distribution and potential for recovery.

As mentioned above, CLG theoretically offers the possibility to convert completely the fuel in the fuel reactor. However, exploiting this possibility is challenging due to the relatively slow kinetics of the steam gasification reaction and the stochastic nature of the mixing in fluidized beds. The mixing can be controlled to some extent and the residence time can be increased, for instance, by placing baffles within the reactor. Reducing the circulation rate of the bed material can enhance the residence time of the fuel, although this parameter cannot be freely adjusted since it is tightly linked to the heat balance. Furthermore, the circulation rate also controls the oxygen transport and the temperature difference between the air and fuel reactors. While increasing the temperature and using catalytic materials can enhance the gasification rate, both cause an increase in the heat demand of the process. The amount of char being transported to the air reactor can be minimized using a so-called "carbon stripper".[38] However, as char is converted, it tends to fragment, creating smaller particles, and this enhances the rate of attrition and, thereby, increases the elutriation of char from the reactor.[39] Thus, this carbon will be lost, together with a small amount of carbon in the form of coking of the bed material, which is burnt in the air reactor. Note that the concentration of CO_2 in the flue gas in CLG is expected to be low, thus incurring a separation cost that will most likely be deemed too high to recover the carbon from the CO_2. Consequently, in a scenario that maximizes carbon recovery, the tar should not be destroyed by combustion in the air reactor, as this would result in an increase in the carbon that is not recovered. The tar must, therefore, be dealt with in some other way.

2.4. CO_2 Utilization within the Plant. As an alternative to sequestration, the CO_2 can be utilized within the plant to synthesize more end product. This requires the addition of H_2, which can be produced from electrolysis of water. This removes the need for CO_2 separation from the syngas, thereby avoiding the related energy cost, although it comes at the expense of the energy demand of the electrolysis, which is an energy-intensive process. CO_2 utilization within the plant synergizes particularly well with the oxyfuel configuration, given that the electrolysis of

https://dx.doi.org/10.1021/acs.energyfuels.0c02781
Energy Fuels 2020, 34, 16187−16200

water produces O_2 as a byproduct of H_2. For the other configurations, however, there is no purpose for that oxygen. The utilization of CO_2 within the plant is not investigated in this work. Nonetheless, it is worth noting that CO_2 utilization does not change the potential for carbon recovery of the various configurations.

3. METHODS

3.1. Plant Layout. The plant layout chosen to compare the DFB gasification configurations is shown in Figure 3. The main section of the plant is the DFB gasification unit, which produces the raw gas that will be refined into the desired range of end products. Prior to its upgrading and the synthesis of end products, the raw gas will be cleaned of constituents that could be deleterious to the downstream processes. The cleaning section is here represented by a filter unit, which separates the fly ash from the gas, and a tar cleaning unit, which scrubs the tar with rapeseed methyl ester (RME). This method of tar cleaning is chosen to reflect its use in the GoBiGas DFB gasifier. The flow of RME in the process is here assumed to be similar to that in GoBiGas, namely, 0.03 MW/MW fuel. Note that, under this assumption, the level of RME feeding is independent of the amount and composition of tar generated by the DFB gasification process. In this work, it is assumed that all of the tar is successfully absorbed by the RME.

As shown in Figure 3 (dashed lines), the mixture of tar and RME can be handled by burning in the combustor, thereby contributing to covering the heat demand. If the heat demand is so high that burning all of the char, as well as the tar and RME mixture, is insufficient, then part of the clean, cold gas can be fed to the combustor, although this is an inefficient and costly solution. Note that, in an actual plant, the off-gases from the synthesis section could also be utilized to cover part of the heat demand. The fly ash removed by the filtration system is also fed to the combustor to recover the elutriated carbon in form of CO_2 in the flue gas. The circulated fly ash also contributes to reducing the need for makeup feeding of the bed material, and it can be a means to maintain high catalytic activity by enhancing the retention of active species.[40] In this work, it is assumed that for all configurations, the fly ash is fed to the combustor; for the air and oxyfuel configurations, the mixture of tar and RME is burnt in the combustor; and in the electrical configuration and the CLG low-*T* case, it is converted in the reformer.

Downstream of the gas cleaning section, the cold gas enters the upgrading section, where its composition will be adjusted to meet the requirement of the synthesis section. In this work, it is assumed that the synthesis is based on the reaction of the hydrogen and carbon monoxide in the syngas only. Therefore, as described in Section 2.1, the gas is reformed to convert all hydrocarbons to H_2 and CO. It is assumed that the reformer can be optimized to produce a gas that contains only H_2, CO, and CO_2. Depending on the desired end product, the syngas needs to have a certain H_2/CO ratio. Consequently, this ratio is adjusted in a WGS reactor. Finally, the CO_2 is removed from the syngas. The synthesis section is represented by a black box, wherein the syngas is completely converted to the end product. The range of possible end products is represented by their apparent C/H ratio, which corresponds to the C/H ratio of the end product corrected by the oxygen content, where two Hs are removed per O removed, in line with the water molecule. In this way, a C/H ratio of 0 corresponds to the production of H_2 and a C/H ratio in the range of 0.25−0.50 represents the range of possible hydrocarbons, with CH_4 at the 0.25 limit and waxes ($-CH_2-$) at the 0.50 limit. Using the apparent C/H ratio, oxygen-containing end products can be fitted to this definition: for instance, methanol as the end product corresponds to a C/H ratio of 0.50.

Concerning the flue gas, cleaning and conditioning must be performed prior to its emission into the atmosphere, despite this not being represented in Figure 3. Depending on the concentration of CO_2 and on the ambition with respect to carbon recovery, a CO_2 separation unit may be required. In this work, CO_2 separation, whether from the flue gas or syngas, is assumed to be carried out using a state-of-the-art scrubbing process based on methyl ethanolamine (MEA). For the flue gas, the heat duty of the reboiler to evaporate the CO_2 from the aqueous amine solution is assumed to be 4 MJ/kg CO_2, which corresponds to a conservative value based on a typical minimum range of 3.6−4.0 MJ/kg CO_2 for 90% CO_2 removal from the flue gas.[41]

For the syngas, the 4 MJ/kg CO_2 value is selected as the maximum expected value of the reboiler heat duty, but the actual value will likely be lower since the CO_2 concentration is expected to be higher than in the flue gas and the pressure above atmospheric pressure, both of which reduce the reboiler duty. For reference, the specific reboiler duty for a syngas with 40 vol % CO_2 at 20 bar is estimated to be 1.9 MJ/kg CO_2, based on the model developed by Garðarsdóttir et al.[42] The reason for the elevated pressure is that the downstream synthesis steps will likely be operated above atmospheric pressure, and compressing the raw gas prior even to its reforming is likely to be the preferred solution since the volume flow will then be lower than that after the reforming step. As the pressure and CO_2 concentration in the syngas increase, other separation techniques than amine absorption may be preferred, but this choice will be the same for all configurations. Regardless of the separation techniques and gas characteristics, it is assumed that all of the CO_2 is removed. Since the goal is to compare the DFB gasification configurations rather than to give a realistic value for the energetic cost of the CO_2 separation, this approach is considered to be reasonable.

3.2. Evaluation Cases. The cases that are compared in this work are described in Table 1. The mass and energy balances of the DFB gasification section are solved based on gas compositions obtained experimentally in the Chalmers DFB gasifier, as shown in Table 2. The reference inert composition, which corresponds to experiments performed at 805 °C with silica sand as the inert bed material, is

Table 1. Descriptions of the Cases Investigated in This Work[a]

configuration	case tag	description
air	air inert	air as the oxidant in the combustor; inert bed material (silica sand)
	air active	air as the oxidant in the combustor; active bed material (aged olivine)
	air full reforming	air as the oxidant in the combustor; gas assumed to be fully reformed to syngas
oxyfuel	oxy active	pure oxygen as the oxidant in the combustor; active bed material (aged olivine)
	oxy full reforming	pure oxygen as the oxidant in the combustor; gas assumed to be fully reformed to syngas
CLG	CLG low-*T*	chemical-looping gasification with ilmenite at 827 °C; the gas composition is that derived from experiments conducted in the Chalmers gasifier
	CLG high-*T*	chemical-looping gasification with ilmenite at 950 °C; gas assumed to be fully reformed to syngas
electrical	El active	electrically heated DFB gasifier; active bed material (aged olivine)

[a]In the second column, the tag by which each case is referred to in the text is indicated.

Table 2. Gas Compositions Produced in the Three Reference Experimental Cases

	unit	reference inert	reference active	reference CLG
H_2	mol/kg daf	9.35	22.01	4.19
CO	mol/kg daf	12.75	7.00	6.12
CO_2	mol/kg daf	5.06	17.12	18.21
CH_4	mol/kg daf	4.68	3.01	2.75
C_2H_4	mol/kg daf	1.44	0.80	0.93
C_2H_2	mol/kg daf	0.10	0.01	0.06
C_2H_6	mol/kg daf	0.19	0.16	0.06
C_3H_6	mol/kg daf	0.10	0.14	0.04
TOC	mol C/mol C fuel	0.087	0.036	0.061

https://dx.doi.org/10.1021/acs.energyfuels.0c02781
Energy Fuels 2020, 34, 16187−16200

used to determine the air-inert case. The reference active composition was obtained at 816 °C with the bed material consisting of olivine that had been activated by its interaction with biomass ash in the DFB gasifier over several days and to which a small amount of K_2CO_3 was initially added to enhance the activation rate. This gas composition is used to determine the active cases of the air, oxyfuel, and electrical configurations. The CLG low-temperature (CLG low-*T*) case is based on an experiment carried out at 827 °C, with ilmenite as the oxygen-carrying bed material. The use of a different gas composition for the CLG configuration reflects the different types of catalytic effects (excluding oxygen transport) that ilmenite and olivine can produce. Note that ilmenite is the most commonly applied natural oxygen carrier[43] and olivine is the catalytic bed material of choice in industrial-scale DFB gasification.[9,10,44]

In addition to the comparison of the four configurations, the air-inert and air-active cases are compared to investigate the differences induced by a change of the bed material from an inert one to a very active one. To determine the mass and energy balances at high temperatures, beyond those that can be achieved in the Chalmers gasifier, a case in which thermodynamic equilibrium is achieved is considered. In this case, referred to as "full reforming" for the air and oxyfuel configurations, the gas is fully reformed (in the gasifier) to a syngas that contains only H_2, CO, and CO_2. This provides reasonable estimates of the mass and energy balances. As the operating temperature increases from the 816 °C of the air and oxy-active cases, the gas composition approaches that of the full reforming cases at high temperatures. Species that diverge from the syngas actually produced at high temperatures might create technical problems, e.g., soot and heavy tar, but they have little impact on the mass and energy balances. The same approach is taken to evaluate the CLG high-*T* case at 950 °C, which corresponds to a more realistic CLG case than the one obtained in the Chalmers gasifier at 827 °C, since such a low temperature is unlikely to allow for complete conversion of the fuel in the fuel reactor.

The gas compositions given in Table 2 are not used directly but are instead adjusted to remove the effects of gasification and oxygen transport. Indeed, the degree of gasification achieved during experiments does not match that set by the heat demand since the heat production in the CFB of the Chalmers DFB gasifier largely exceeds this requirement. The H_2 and CO yields are, therefore, adjusted to eliminate the effect of gasification. Concerning the oxygen transport, the availability of oxygen in the CFB is also much higher than required by the heat balance in an actual DFB gasification unit. Therefore, the oxygen transport measured in the Chalmers DFB gasifier is considered to be unrealistic, so its contribution to the gas composition is removed by increasing the H_2 and CO yields and decreasing the CO_2 yield, assuming that only H_2 and CO reacted with the transported oxygen, in equal parts. Accounting for the oxygen transported, the priority is given to the H_2 and CO formed from gasification of char, before the H_2 and CO formed from devolatilization and volatile reactions.

Therefore, there are two possibilities for the adjustment of the gas composition, depending on how the oxygen transported compares with the oxygen required for oxidation of the H_2 and CO formed from char gasification: (1) If it is lower, then the H_2 and CO yields are decreased; and (2) if it is higher, then the H_2 and CO yields are increased to account for the oxidation of volatiles. The CO_2 yield is then determined from the carbon balance since the amount of carbon in the permanent gas is known. The heat demand is then used to determine the achievable degrees of gasification for the air and oxyfuel configurations (albeit not from the kinetic standpoint), as well as the levels of oxygen transport for the CLG cases.

The assumptions mentioned in the previous paragraph are deemed reasonable, given that H_2 and CO are the species most likely to react with the transported oxygen, as explained in Section 2.3.2. Furthermore, devolatilization is more likely to occur on the bed surface,[45,46] especially at larger scales. Additionally, the design of most industrial-scale DFB gasifiers, which are based on the Güssing gasifier, circulate the bed to the combustor through the bottom of the gasifier, thereby forcing the char to go into the bed instead of staying on top of it, thus increasing the contact between gasification products and the bed material. Therefore, the gasification products are more likely to be oxidized than the volatiles.

3.3. Evaluation of the CO_2 Separation Sections. The energy demand for desorption of the CO_2 from the saturated MEA solution can be determined based on the assumed specific heat demand of the desorption step per unit mass of CO_2 and based on the levels of carbon recovery in the flue gas and syngas. The temperature level of the required heat load is low, which means that it can be covered in part or entirely by heat integration. A complete assessment of the available heat sources and their temperature levels is beyond the scope of this paper and depends to a large extent on the plant design, thus it cannot be generalized. Nonetheless, the main heat sources of the plant will be the flue gas and raw gas from the DFB unit. Therefore, a comparison of the potentials for heat extraction from these sources with the reboiler heat duty can indicate whether the demand can be covered internally or whether additional energy will be required. The investment cost of the separation equipment, reflecting mainly the size of the absorption and desorption columns, can be qualitatively compared and discussed between the DFB configurations by comparing the number of streams from which CO_2 must be extracted (one or two, depending on whether the CO_2 from the flue gas is recovered) and the CO_2 concentrations in these streams. The electrical energy demand, which is related to the production of pure oxygen for the oxyfuel configuration and direct heating for the electrical configuration, is also of interest for the evaluation of CO_2 separation, as it corresponds to the energy associated with avoiding the need for separation of CO_2 from the flue gas stream.

In this work, the calculation of the heat recovery potential assumes that the gas is cooled to 160 °C and that the tar is scrubbed off the raw gas using RME. Although other approaches may allow for higher heat recovery, this solution is chosen to ensure the comparability of the cases. Furthermore, this is the approach chosen in the GoBiGas DFB plant, which is the reference for most of the assumptions made. Besides, this approach relies on cold fly ash removal and gas cleaning technologies, which are easier to implement than hot technologies.

3.4. Experimental Section. *3.4.1. Chalmers DFB Gasifier.* The heat and mass balances in this work are based on gas compositions obtained from the Chalmers DFB gasification system. The gasifier is a 2−4-MWth bubbling fluidized bed, which was retrofitted to a 12 MWth CFB boiler. An extensive description of the unit can be found elsewhere.[47]

3.4.2. Measurement System. The measurement system of the Chalmers DFB gasifier has been extensively described by Berdugo Vilches et al.[48] Only a brief summary is given here. A slipstream from the raw gas is extracted and filtered to remove the particulate matter. From that slipstream, two substreams are produced. The first substream is quenched with cold isopropanol to remove the tar and moisture and is then sent to a microgas chromatograph, where the composition of the dry gas is analyzed. The tar is sampled from that same substream, prior to its quenching, using the solid-phase adsorption method, which has been described by Israelsson et al.[49] The elution of the adsorption columns and the analysis of the eluate are described elsewhere.[48,49] The second raw gas substream is cracked in a high-temperature reactor (HTR) at 1700 °C to produce a syngas that consists exclusively of H_2, CO, CO_2, and H_2O. This enables the quantification of the degree of gasification, as well as of the amount of carbon in the form of hydrocarbons with more than three carbon atoms, referred to as "TOC" in Table 2. The HTR and its use in the elucidation of the carbon balance have been described by Israelsson et al.[50] The dry, cold gases from both substreams are analyzed in microgas chromatographs of the same model with similar columns. The gas species measured are H_2, He, N_2, CO, O_2, CO_2, CH_4, C_2H_2, C_2H_4, C_2H_6, C_3H_6, C_3H_8, and H_2S. Note that the presence of helium in the gas is due to its use as a tracer in the gasifier, which enables the quantification of the carbon distribution.

3.4.3. Materials. The results presented in this work are based on the gasification of wood pellets, the characteristics of which are assumed to be similar to those of the wood pellets used to obtain the gas compositions given in Table 2. The proximate analysis, ultimate analysis, and calorific value of the wood pellets considered in this work are presented in Table 3. The compositions of the reference bed materials (silica sand, olivine, and ilmenite) are given in Table 4. Note

https://dx.doi.org/10.1021/acs.energyfuels.0c02781
Energy Fuels 2020, 34, 16187−16200

Table 3. Proximate Analysis, Ultimate Analysis, and Calorific Value of the Wood Pellets Used in This Work[a]

proximate analysis				ultimate analysis			calorific value
moisture	ash	fixed carbon	volatile matter	C	H	O	LHV
wt % as received	wt % dry	wt % dry	wt % dry	wt % daf	wt % daf	wt % daf	MJ/kg dry
8.0	0.4	16.0	83.6	50.5	6.2	43.3	18.8

[a]"daf" refers to the dry ash-free fuel.

Table 4. Elemental Compositions (Mass Percentages) of the Reference Bed Materials in This Work

	silica sand	olivine	ilmenite
Si	46.37	19.49	0.14
Fe	0.04	5.18	34.25
Mg		29.91	0.56
Al	0.09	0.24	0.20
Ti			30.27
Mn			0.76
Cr		0.21	0.17
V			0.11
rest[a]	53.50	44.96	33.54

[a]Refers to minor and trace metals and oxygen.

that these are the compositions of the fresh materials, before any interaction with ash components from the fuel. This is, therefore, not representative of the state of the bed materials in the DFB gasifier that resulted in the gas compositions given in Table 2. This is true, in particular, for olivine, which can be expected to have interacted strongly with the ash components. The results of DFB gasification experiments in the Chalmers system using these bed materials have been reported previously.[51−53]

3.5. Additional Assumptions. This section describes three additional assumptions that were employed when determining the cases described above. As mentioned in Section 2.2, recirculation of the flue gas is necessary to maintain a low flame temperature in the oxyfuel configuration. In this work, the required rate of flue gas recirculation is set so that the adiabatic flame temperature of the oxyfuel configuration is the same as that of the air configuration. This results in recirculation of about 75% of the flue gases. The flue gases produced in the oxyfuel configuration will still contain some oxygen since the combustor is operated at an excess oxygen ratio of 1.2, which is a value selected for comparability with the other configurations, for which the excess oxygen ratio is also 1.2. The choice of this value results in O_2 concentrations in the dry flue gas of about 5%, which is comparable with values obtained in oxyfuel combustion installations.[31] To react the remaining O_2 in the flue gas, a postcombustion step is introduced. In this step, syngas is preferred to raw gas to avoid having unburnt hydrocarbons in the postcombustion gases.

A final key assumption concerns the amount of char elutriated due to its erosion and fragmentation during conversion in the gasifier. It is assumed that this level of char elutriation accounts for 10% of the carbon in the char. Therefore, the maximum possible conversion rate is 90%. The choice of this value is arbitrary, as the actual value will be device- and fuel-specific. It is set to 10% to represent the fact that carbon is found in relatively high amounts in the product gas ash from DFB gasifiers,[8,10] part of which can be expected to be in the form of char. Nonetheless, this choice has little impact on the results, as varying the level of char elutriation between 1 and 30% of the carbon in the char resulted in only limited changes in the carbon and energy balances.

Table 5 summarizes the key assumptions that differ between cases, namely, whether RME is introduced to clean the raw gas of tar, whether the mixture of tar and RME is combusted, and whether the char conversion is fixed by the heat demand or assumed complete. Feeding

Table 5. Summary of the Key Assumptions That Differ between Cases[a,b]

		assumptions		
configuration	case tag	RME	combustion of tar−RME mixture	char conversion
air	air inert	yes	yes	fixed by heat demand
	air active	yes	yes	
	air full reforming	no	n.a.	
oxyfuel	oxy active	yes	yes	
	oxy full reforming	no	n.a.	
CLG	CLG low-T	yes	no	complete (but limited by elutriation)
	CLG high-T	no	n.a.	
electrical	El active	yes	no	

[a]n.a., not applicable. [b]The RME assumptions indicate whether RME input is necessary or not.

of RME is necessary in all cases except those that assume that the gas is fully reformed in the gasifier, i.e., the air full reforming, oxy full reforming, and CLG high-T cases. The mixture of tar and RME is assumed to be converted in the reformer instead of being burnt in the combustor in the carbon-free heat production configurations, i.e., the CLG low-T and El-active cases.

4. THEORETICAL CONSIDERATIONS

4.1. Theoretical Yields. The purpose of this section is to provide a theoretical basis for the conversion of fuel to a given end product by reaction with steam and to detail how an actual DFB gasification process will deviate from the theory. The conversion of biomass with composition CH_yO_z to produce an end product CH_iO_j using steam can be written as the following conceptual reaction

$$CH_yO_z + a\cdot H_2O \rightarrow b\cdot CH_iO_j + c\cdot CO_2 \quad \text{(R1)}$$

From this equation, it is clear that the production of the end product is accompanied by the production of a certain amount of CO_2. The theoretical yields of carbon recovered as the end product and the CO_2 that can be produced without further synthesis of the CO_2 produced, referred to as b and c, respectively, can be defined as follows

$$b = \frac{1 + \frac{y}{4} - \frac{z}{2}}{1 + \frac{i}{4} - \frac{j}{2}}$$

$$c = \frac{\left(\frac{i}{4} - \frac{j}{2}\right) - \frac{y}{4} + \frac{z}{2}}{1 + \frac{i}{4} - \frac{j}{2}}$$

Actual DFB gasification deviates from the theoretical case in a number of ways. First, the energy demand for the reactions and the heating of the fuel is met by combusting part of the char, resulting in less available carbon for the syngas. To burn that char, an oxidant is needed, which incurs a heat demand to bring it to the combustor temperature since it is unlikely that there are heat sources in the process that can be used to preheat the oxidant to that temperature. Similarly, it is unlikely that the steam will be preheated to the gasifier temperature, incurring an additional energy demand. Furthermore, the gasification and combustion reactor will entail some losses due to the imperfection of the construction and insulation. The fuel

https://dx.doi.org/10.1021/acs.energyfuels.0c02781
Energy Fuels 2020, 34, 16187−16200

hopper and the feeding system must be inertized, which can be accomplished with CO_2. However, this also increases slightly the heat demand of the gasifier. Finally, the circulating bed material will lose some heat between the combustor and the inlet of the gasifier, which means that the combustor must be operated at a higher temperature (generally about 50 °C higher) than the target temperature of the gasifier. All of these deviations from the ideal situation result in an increased heat demand of the process. However, there is also a deviation that causes a decrease in the heat demand relative to the theoretical case, with all else being equal: the extents of the reactions in the gasifier. The kinetics of the reaction in the gasifier means that the gas will be much more complex than the theoretical syngas. Besides, the gasification of char is a slow process, the completion of which is challenging in a DFB gasifier due to the circulating bed limiting the residence time.

4.2. Choice of Operating Temperature. In this work, the DFB gasification configurations are compared at similar gasification temperatures for the air-inert, air-active, oxy-active, El-active, and CLG low-*T* cases (see Section 3.2). However, the chosen operating temperature for the gasifier will differ between the configurations. The choice of operating temperature is complex and depends on many factors. The temperature is expected to affect the carbon distribution of the process since it directly influences the heat demand of the DFB gasification process. Furthermore, it affects the kinetics of the reactions that occur in the gasifier, as well as their equilibrium, although for most reactions equilibrium is not expected to be reached in the gasifier due to limited residence times. The energy efficiency of the plant is also expected to be impacted since a change in the carbon distribution will likely change the energy demands of the upgrading and synthesis steps, as well as of the CO_2 separation process. Beyond the aspects of carbon recovery and energy efficiency, some practical considerations affect the choice of temperature. With higher temperatures, the risk of agglomeration of the bed material increases, as does the risk of fouling of the heat exchange surface, since heavier, high-boiling-point tar species are formed at higher temperatures.[16] Finally, the degree of char gasification that the DFB gasifier can sustain will directly determine the gasifier temperature. Indeed, at higher temperatures, the gasification rate increases but the increase in heat demand requires more char to be combusted, which means that the system will equilibrate to a lower temperature unless cold gas is burnt to maintain that temperature at that degree of gasification.

5. RESULTS

5.1. Carbon Distribution. The carbon distributions of the various DFB configurations are shown in Figures 4 and 5. Figure 4 shows the levels of carbon in the form of CO_2 in the syngas, while Figure 5 shows the carbon in the end product. Note that the carbon distribution is based on the carbon input of the fuel. However, for the cases in which RME is needed to remove the tar, i.e., all cases except the CLG high-*T* case and the theoretical curve (reaction R1), this introduces a slight discrepancy in the figure since the total amount of carbon fed to the system differs slightly. Figure 6 shows the breakdown of the total heat demands of the DFB gasification processes, as well as the carbon intensities of the various cases. The carbon intensity refers to the CO_2 produced in both the flue gas and raw gas as a result of the heat production method. For CLG, this corresponds to the CO_2 formed in the raw gas by oxidation of carbon-containing species by the oxygen transported to the fuel reactor.

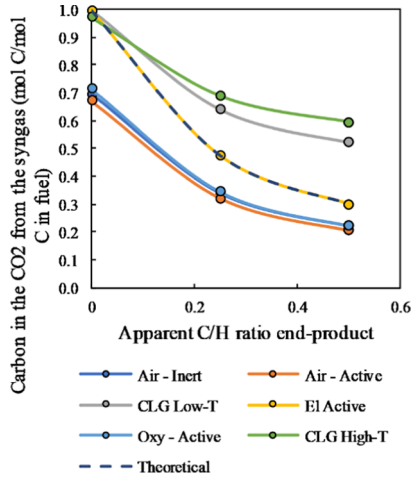

Figure 4. Carbon in the form of CO_2 in the syngas versus the apparent C/H ratio of the end product. The dashed line represents the theoretical amount of carbon in the form of CO_2, according to reaction R1. The profiles shown in the graph for the air-inert and oxy-active cases are overlapping.

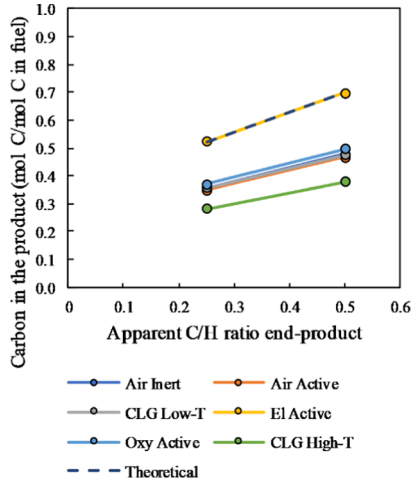

Figure 5. Carbon in the form of end product versus the apparent C/H ratio of the end product, for C/H ratios in the range of 0.25−0.50. The dashed line represents the theoretical amount of carbon in the form of CO_2, according to reaction R1. The profiles in the graph for the air-inert and air-active cases are overlapping.

Figure 5 shows that there is little difference between the various cases regarding the carbon in the form of end product, with the exceptions of the electrical configuration and the high-temperature CLG case. The CLG high-*T* case shows the lowest level of carbon recovered as the end product, which is explained by its higher heat demand, due to the higher temperature as well as the more intense heat of reaction (gasification and volatile reforming). Nonetheless, there is little difference between the low- and high-temperature CLG cases. The electrical configuration, as expected, produces a carbon distribution close to that of the stoichiometry of reaction R1, as it is unaffected by the "loss" that corresponds to the requirement of fulfilling the heat demand. The only discrepancy from the theoretical curve results from the RME fed and the elutriation of 10% char.

The use of the CLG configuration leads to the highest level of CO_2 in the syngas and the lowest level (albeit only slightly so for the CLG low-*T* case) of recovery of carbon as the end product, despite allowing for complete fuel conversion and not requiring

https://dx.doi.org/10.1021/acs.energyfuels.0c02781
Energy Fuels 2020, 34, 16187−16200

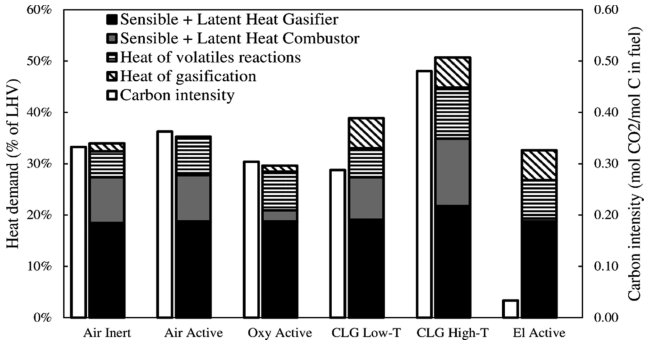

Figure 6. Contributions to the total heat demands of the various cases and the carbon intensities of the heat production methods. The latter represent the amounts of CO_2 produced in both the flue and raw gases due to the production of heat. The carbon intensity is represented by a white bar next to the stacked bars, and its values are displayed on the right vertical axis.

direct combustion of char or gas. This is the result of two phenomena: (1) bed oxidation drives the transport of oxygen to the fuel reactor, which in turn causes the conversion of carbon in the products to CO_2, and (2) the high degree of gasification entails a higher heat demand than is seen in the air and oxyfuel configurations. As shown in Figure 6, this results in the carbon intensity in the CLG configuration being similar to or even higher than those in the air and oxyfuel configurations.

5.2. CO_2 Separation. Figure 7 shows the values of the energy demands and sources relevant to the evaluation of the CO_2 separation step, according to Section 3.3. The reboiler heat duties for separation of the CO_2 from the syngas, for end products with C/H ratios of 0, 0.25, and 0.50, are shown, distinguishing between the reboiler duty for the separation of CO_2 from the flue gas (continuous boxes) and the energy demand for the separation of CO_2 from the syngas (dashed boxes). For reference, the energy demand for CO_2 separation from a syngas with 40 vol % CO_2 at 20 bar using MEA absorption is indicated by a black dot. It is clear from the figure that the reboiling of the amine solution represents a major share of the overall energy demand of the plant, as it can be comparable to the total heat demand of the DFB unit (see Figure 6) depending on the cost for energy separation of the syngas. Comparing the two air cases, it is apparent that the extents of the reactions inside the gasifier have only weak impacts on the reboiler heat duty and the available heat. Similarly, the two CLG cases show little difference from each other. Given their large amounts of available heat, the CLG cases are likely to be in a position to benefit from heat integration to cover their reboiler heat duties.

The energy demand associated with oxygen production in the oxyfuel configuration is rather low and leads to a significant drop in the total reboiler heat duty since the postcombustion flue gas does not require further CO_2 separation before compression and sequestration. It should be noted that while the oxyfuel configuration is advantageous from the energy standpoint, it may not be from an exergy perspective since the value of the electric energy used is much higher than the heat required by the reboiler. In the case of the electrical configuration, the electrical heat demand to heat the bed material is high, reaching about 30% of the energy input with the fuel. Furthermore, this case has the lowest available heat, owing to the low gas flow in the combustor (relative to all the other cases). Depending on the energy requirement for CO_2 separation from the syngas, heat integration may not be sufficient to cover the reboiler heat duty and heat might need to be provided electrically, thereby decreasing the overall energy efficiency of the plant.

The reboiler heat duties shown in Figure 7 for the various cases are only measures of the energetic cost of separating the CO_2. Thus, they do not inform as to the costs related to the dimensions of the separation columns and to the levels of MEA needed. These aspects can be indirectly assessed by looking at the concentrations of CO_2 in the syngas and flue gas, as shown in

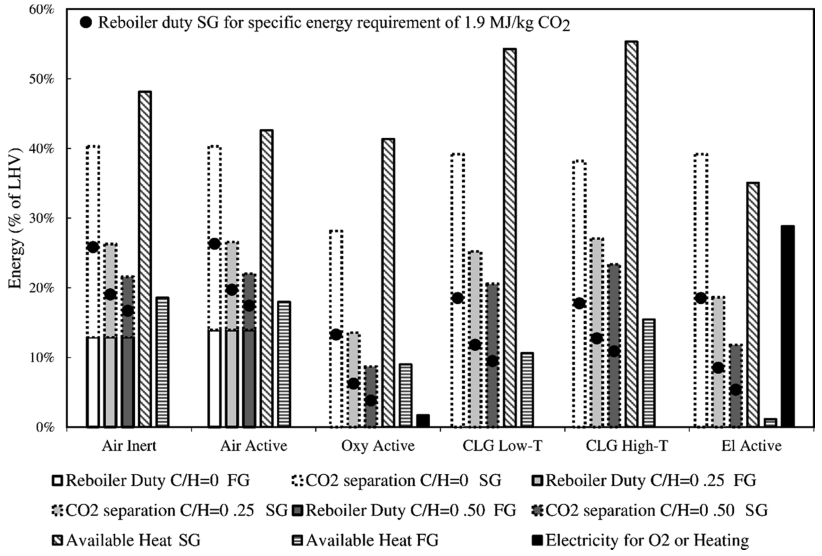

Figure 7. Energy demand for CO_2 separation for the various end products, as compared with the available heats (latent and sensible) from the raw gas (RG) and flue gas (FG), for the various DFB configurations. The electricity demands for the production of pure oxygen (oxyfuel configuration) and for direct heating (electrical configuration) are also shown. The reboiler duties for the separation of the CO_2 from the flue gas are shown in continuous boxes, whereas the energy demands for the separation of the CO_2 from the syngas are shown in dashed boxes. The black dot represents the energy demand for CO_2 separation from the syngas gas when MEA absorption is used, for a syngas with 40% CO_2, at 20 bar, corresponding to a specific energy requirement of 1.9 MJ/kg CO_2.

https://dx.doi.org/10.1021/acs.energyfuels.0c02781
Energy Fuels 2020, 34, 16187−16200

Figures 8 and 9, respectively. It can be seen from Figure 8 that the concentration of CO_2 in the syngas is similar for all cases,

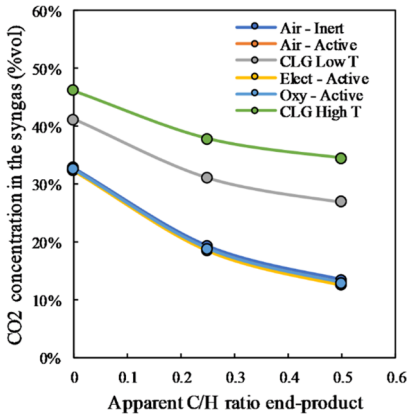

Figure 8. CO_2 concentrations in the syngas versus the apparent C/H ratios of the end products for the different configurations. The profiles shown in the graph for the air-inert, air-active, oxy-active, and El-active cases are overlapping.

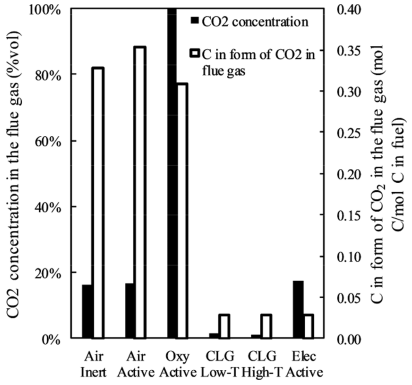

Figure 9. CO_2 concentrations (black bars) and fractions of carbon in the form of CO_2 in the flue gas (white bars, relative to the carbon in the fuel) for the different configurations.

except for the CLG cases, which result in higher concentrations of CO_2. Based on this finding, the CLG configuration will have a lower specific energy requirement for CO_2 separation (per unit mass of CO_2 removed), meaning that, for a given syngas pressure, the value of the energy for CO_2 separation from the syngas shown in Figure 7 will be lower than those for the other cases. However, this is probably mainly true at the higher C/H end product target since the increase in specific heat of CO_2 desorption with an increment in CO_2 concentration decreases at higher concentrations. As noted in Section 3.1, when higher pressures are required by the downstream synthesis section, other separation technologies than amine absorption may be preferred, for which the specific energy requirement for CO_2 separation may be lower and heat integration not a possibility.

As shown in Figure 9, the CO_2 concentration in the flue gas is comparable to that of the CFB combustors with the air and electrical configurations. Note that the CO_2 concentration in the electrical configuration is relatively high, whereas the absolute amount of carbon in the form of CO_2 is low. As a consequence, the investment cost related to building a second scrubber may be deemed too high. For this reason, the CO_2 from the flue gas was considered to be not recovered in the electrical configuration. In the oxyfuel configuration, the postcombustion flue gas does not require further CO_2 separation, as mentioned previously. For the CLG cases, the CO_2 concentration is so low that separation will be too costly, from both the investment and energy standpoints.

5.3. Choice of Operating Temperature. Figure 10 shows the impacts of increasing the operating temperature from 810 °C (low *T*) to 950 °C on the carbon distribution, reboiler heat duty, and electrical demand for the air and oxyfuel configurations. For both of these configurations, operating at a higher temperature decreases the amount of carbon recovered in the end product.

Despite some small differences between the configurations, it appears that an increase in temperature as large as 140 °C does not significantly affect the carbon distribution. The energy demand of the CO_2 separation step is unlikely to be significantly impacted, given that the reboiler heat duty is scarcely affected by the higher operating temperatures. Nonetheless, the higher temperature levels of the raw gas and flue gas from the DFB gasifier mean that there is greater potential for heat recovery and, thereby, heat integration. It is, however, difficult to justify operating at high temperatures, given that this entails an increased risk of operational issues, such as an increased risk of

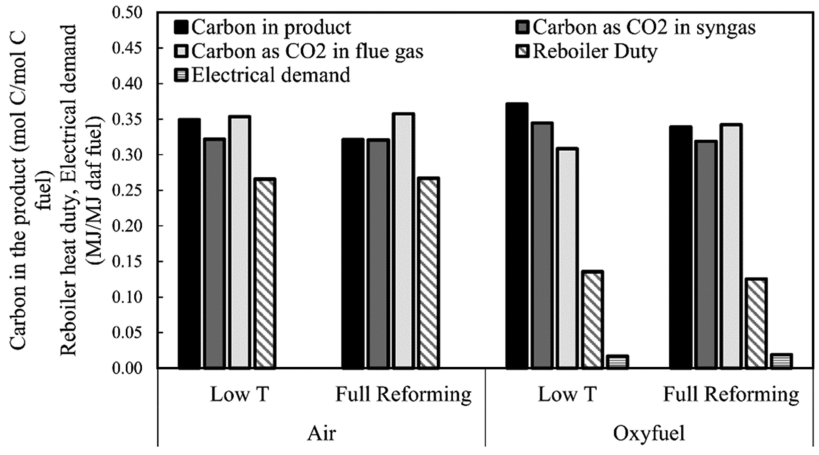

Figure 10. Effects of an increase in operating temperature on the carbon distribution, reboiler heat duty, and electrical demand for the air and oxyfuel configurations. Low *T* refers to the air/oxy-active case at 810 °C. Full reforming refers to a case in which the gas is fully reformed at 950 °C, as described in Section 3.2. Note that the carbon distribution is here based on the total carbon input, i.e., including the RME. The results shown are for a C/H ratio of 0.25.

https://dx.doi.org/10.1021/acs.energyfuels.0c02781
Energy Fuels 2020, 34, 16187−16200

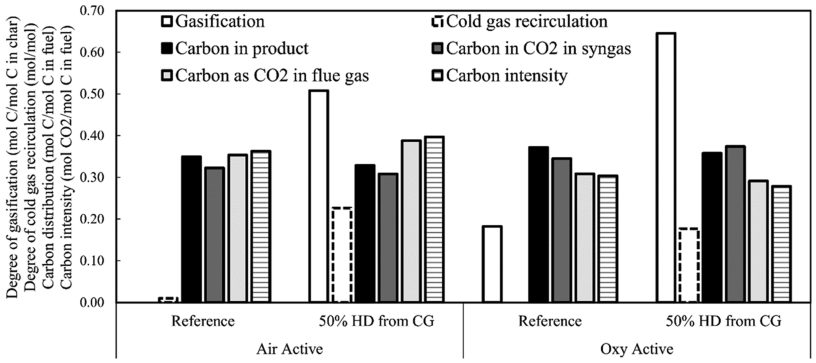

Figure 11. Impacts on the degree of gasification, degree of cold gas recirculation, carbon distribution, and carbon intensity of covering 50% of heat demand by combusting cold gas, as compared with the reference, i.e., combustion of the tar−RME mixture, fly ash, and char only. The carbon intensity here refers to the amount of CO_2 produced in both the flue gas and raw gas due to the heat production method. The results shown are for a C/H ratio of 0.25.

agglomeration and, potentially, an increase in fouling from tar condensation. Higher temperatures promote the formation of heavier tar species with higher boiling points but also decrease the total amount of tar, such that the net effect on fouling risks will depend on the temperature level and the type of fuel. Furthermore, the heat balance requires the combustion of all of the char produced from the fuel, which at such high temperatures would be challenging since the gasification rates would be high. This would necessitate either high circulation rates to keep the fuel residence time low, which would severely increase the energy demand from the air fan, or the combustion of more cold gas to cover the heat demand at a high degree of gasification. Overall, there appears to be no incentive for the operation of the air and oxyfuel configurations at high temperatures.

This result is in accordance with that reported by Alamia et al., who modeled DFB gasification based on data acquired from the GoBiGas plant. The authors found that operating the gasifier at a lower temperature led to an increase in the cold gas efficiency, i.e., the ratio of energy in the cold gas to the energy content of the fuel. However, it should be noted that in the GoBiGas DFB gasifier, the level of recirculation of cold gas to the combustor is significant and that a decrease in temperature only led to a decrease in cold gas recirculation without affecting the degree of gasification.[54]

5.3.1. Covering the Heat Demand: Char Combustion versus Cold Gas Combustion. Even when operated at 810 °C, the heat demand of the air-active DFB process is such that no gasification is allowed and all of the char needs to be combusted (Figure 6). Nevertheless, some gasification is expected to occur, especially since catalytic species are introduced, as biomass ash and additives to reduce the amount of tar and, consequently, reduce the risk of fouling in the cooling sections. Therefore, some of the cold gas will need to be combusted. The impact of the combustion of cold gas, as compared with the combustion of char, is shown in Figure 11, comparing a case in which, at 810 °C, 50% of the heat demand is provided by the combustion of cold gas with the reference case, which is based on prioritizing the combustion of char. For both the air-active and oxy-active cases, the degree of gasification, degree of cold gas recirculation, carbon distribution, and carbon intensity of the heat production are shown.

Covering half of the heat demand through the combustion of cold gas allows reaching a degree of gasification of 50% for the air configuration and 65% for the oxyfuel configuration. These targets are unlikely to be achievable at 810 °C. However, the goal here was to exaggerate the degree of cold gas recirculation to assess the impact on the carbon balance. As can be seen in Figure 11, for both configurations, combusting the cold gas leads to a slight decrease in the recovery of carbon as the end product, which is a consequence of the increased heat demand that arises from the increased degree of gasification. Overall, these results indicate that the combustion of cold gas (as compared with the combustion of char) is detrimental, albeit less so for the oxyfuel configuration, and the effect will be more pronounced at higher temperatures. This suggests that, at low temperatures of operation, one should strive to limit the char gasification rate.

6. FEASIBILITY LEVELS OF THE CARBON-FREE HEAT PRODUCTION CONFIGURATIONS

The main obstacle facing the carbon-free heat production configurations is the very aspect that makes them so attractive in the first place, namely the potential to achieve complete conversion of the fuel in the gasifier/fuel reactor. Due to the interdependence of numerous parameters in the DFB setup, achieving complete conversion via optimization of the operating parameters is challenging. Moreover, the conditions that allow for complete conversion can be so extreme to increase the risk of operational issues. For instance, for both the CLG and electrical configurations, high temperatures may lead to agglomeration and may, when combined with alkali for catalysis, increase the risk of corrosion. This is especially troublesome for the structural integrity of the tube banks in the electrical configuration. Nevertheless, due to the stochastic nature of the mixing in the fluidized bed, transport of some char to the combustor/air reactor is unavoidable. Consequently, the use of a carbon stripper to eliminate or minimize that loss is necessary. Instead of aiming for complete conversion, char could be considered as a product of the plant.

Achieving complete conversion in the gasifier/fuel reactor may be simpler when converting carbon sources that produce little char. Fortunately, the primary source of carbon in the future carbon system will be carbon-containing waste, a large fraction of which is expected to be polyolefinic in nature. Therefore, under gasification conditions, these wastes are expected to produce little char, the level of which could be insufficient to cover the heat demand in the air and oxyfuel configurations but would be much more suitable than biomass for the carbon-free heat production DFB configurations. Furthermore, the amount of elutriated char would be greatly

https://dx.doi.org/10.1021/acs.energyfuels.0c02781
Energy Fuels 2020, 34, 16187−16200

decreased, thereby reducing carbon loss through the flue gas. Still, plastics tend to form more and heavier tars than biomass,[55,56] and this may result in higher levels of soot. Nonetheless, polyolefin-rich waste should be a suitable fuel for conversion using the CLG and electrical configurations.

Another challenge with the CLG configuration is related to the oxidation of the gases in the fuel reactor. As shown in Figure 5, this leads to the lowest carbon recovery in the end product. An advantage of CLG is its potential to facilitate carbon recovery by not producing CO_2 in the flue gas and allowing higher-level conversion in the fuel reactor. However, there is still a significant energy requirement for the separation of the CO_2 from the syngas, especially considering that most of the carbon is recovered in the form of CO_2 in the syngas. Nevertheless, as shown in Figure 7, the energy demand for CO_2 separation is lower than for the regular DFB case and comparable to the oxyfuel configuration. Furthermore, there is a difference from the investment cost perspective since the regular DFB case assumes separation of CO_2 in both the flue gas and syngas, whereas only the syngas is treated in the CLG configurations.

7. CONCLUSIONS

Four DFB gasification configurations, air, oxyfuel, CLG, and electrical, are compared on the basis of the carbon distributions that they produce and the potentials for carbon recovery that result from those distributions. In addition, their energy demands for CO_2 separation are evaluated through their reboiler heat duties and their potentials for heat integration. Comparing the configurations shows that the air and oxyfuel configurations lead to similar carbon distributions. The impact of using an inert or active bed material, even though critical for operability, is found to be low for the overall carbon distribution. The CLG configuration leads to the lowest level of recovery of carbon as the end product and the highest level of recovery of CO_2 in the syngas. The oxyfuel and CLG configurations show the lowest energy demand for CO_2 separation, although it is not possible from this work to state which of the two exhibits the lowest. For the oxyfuel configuration, the difference with the other cases (except the CLG ones) is greater than the energy required to produce pure oxygen. The electrical configuration entails reboiler heat duties that are comparable to those of the other configurations, albeit with a lower potential for heat recovery. Nonetheless, from an investment cost perspective, the CLG and electrical configurations are favored over the air configuration, as they require only one scrubbing column, for the syngas only.

Concerning the choice of operating temperature, there is no incentive to operate the gasifier at high temperatures for the air and oxyfuel configurations, as this does not lead to any significant change in the carbon distribution but instead leads to increased heat demand. If recovery of an end product is the main goal, then operation at low temperatures is preferred. Overall, for the air and oxyfuel configurations, there is no driver to increase the degree of gasification but instead there is reason to limit it and operate at low temperatures.

The carbon-free heat production configurations need to accomplish complete conversion in the gasifier/fuel reactor. Thus, these configurations are more suited to the extraction of carbon from low-char-forming sources, such as plastic waste, rather than from biomass. The CLG configuration only makes sense if the complete conversion can be achieved. Otherwise, any process that produces heat by oxidizing both char and the bed material only leads to decreased carbon recovery as CO_2 in the raw gas (and downstream in the syngas), as compared with the ideal CLG case, and a lower concentration of CO_2 in the flue gas compared with regular DFB gasification, leading to a more challenging CO_2 separation step.

AUTHOR INFORMATION

Corresponding Author

Sébastien Pissot − *Division of Energy Technology, Department of Space, Earth, and Environment, Chalmers University of Technology, 412 96 Göteborg, Sweden;* orcid.org/0000-0003-0040-8340; Phone: +46317725253; Email: pissot@chalmers.se

Authors

Teresa Berdugo Vilches − *Division of Energy Technology, Department of Space, Earth, and Environment, Chalmers University of Technology, 412 96 Göteborg, Sweden;* orcid.org/0000-0001-8403-6868

Henrik Thunman − *Division of Energy Technology, Department of Space, Earth, and Environment, Chalmers University of Technology, 412 96 Göteborg, Sweden*

Martin Seemann − *Division of Energy Technology, Department of Space, Earth, and Environment, Chalmers University of Technology, 412 96 Göteborg, Sweden*

Complete contact information is available at: https://pubs.acs.org/10.1021/acs.energyfuels.0c02781

Notes

The authors declare no competing financial interest.

ACKNOWLEDGMENTS

This work was supported by Göteborg Energi AB, Akademiska Hus, and the Swedish Energy Agency. The authors thank research engineers Jessica Bohwalli, Johannes Öhlin, and Rustan Hvitt for their assistance with the experimental work and Maximillian Biermann for his help with the estimation of the specific reboiler duty for the MEA absorption from the syngas. The authors also thank Vincent Collins for his skillful editing of the manuscript.

REFERENCES

(1) Van Ewijk, S.; Stegemann, J. A.; Ekins, P. Global Life Cycle Paper Flows, Recycling Metrics, and Material Efficiency. *J. Ind. Ecol.* **2018**, *22*, 686−693.

(2) Masson-Delmotte, V.; Zhai, P.; Pörtner, H.-O.; Roberts, D.; Skea, J.; Shukla, P. R.; Pirani, A.; Moufouma-Okia, W.; Péan, C.; Pidcock, R. et al. *Global Warming of 1.5 °C. An IPCC Special Report*; IPCC, 2018.

(3) Thunman, H.; Berdugo Vilches, T.; Seemann, M.; Maric, J.; Vela, I. C.; Pissot, S.; Nguyen, H. N. T. Circular Use of Plastics-Transformation of Existing Petrochemical Clusters into Thermochemical Recycling Plants with 100% Plastics Recovery. *Sustainable Mater. Technol.* **2019**, *22*, No. e00124.

(4) Fuss, S.; Canadell, J. G.; Peters, G. P.; Tavoni, M.; Andrew, R. M.; Ciais, P.; Jackson, R. B.; Jones, C. D.; Kraxner, F.; Nakicenovic, N.; et al. Betting on Negative Emissions. *Nat. Clim. Change* **2014**, *4*, 850−853.

(5) Sikarwar, V. S.; Zhao, M.; Clough, P.; Yao, J.; Zhong, X.; Memon, M. Z.; Shah, N.; Anthony, E.; Fennell, P. An Overview of Advances in Biomass Gasification. *Energy Environ. Sci.* **2016**, *9*, 2939−2977.

(6) Uddin, M. N.; Techato, K.; Taweekun, J.; Mofijur, M.; Rasul, M. G.; Mahlia, T. M. I.; Ashrafur, S. M. An Overview of Recent Developments in Biomass Pyrolysis Technologies. *Energies* **2018**, *11*, No. 3115.

(7) Al-Salem, S. M.; Lettieri, P.; Baeyens, J. Recycling and Recovery Routes of Plastic Solid Waste (PSW): A Review. *Waste Manage.* **2009**, *29*, 2625−2643.

(8) Thunman, H.; Seemann, M.; Berdugo Vilches, T.; Maric, J.; Pallares, D.; Ström, H.; Berndes, G.; Knutsson, P.; Larsson, A.; Breitholtz, C.; et al. Advanced Biofuel Production via Gasification – Lessons Learned from 200 Man-Years of Research Activity with Chalmers' Research Gasifier and the GoBiGas Demonstration Plant. *Energy Sci. Eng.* **2018**, *6*, 6−34.
(9) Kuba, M.; Kraft, S.; Kirnbauer, F.; Maierhans, F.; Hofbauer, H. Influence of Controlled Handling of Solid Inorganic Materials and Design Changes on the Product Gas Quality in Dual Fluid Bed Gasification of Woody Biomass. *Appl. Energy* **2018**, *210*, 230−240.
(10) Kirnbauer, F.; Koch, M.; Koch, R.; Aichernig, C.; Hofbauer, H. Behavior of Inorganic Matter in a Dual Fluidized Steam Gasification Plant. *Energy Fuels* **2013**, *27*, 3316−3331.
(11) Maric, J.; Berdugo Vilches, T.; Thunman, H.; Gyllenhammar, M.; Seemann, M. Valorization of Automobile Shredder Residue Using Indirect Gasification. *Energy Fuels* **2018**, *32*, 12795−12804.
(12) Pissot, S.; Berdugo Vilches, T.; Maric, J.; Cañete Vela, I.; Thunman, H.; Seemann, M. Thermochemical Recycling of Automotive Shredder Residue by Chemical-Looping Gasi Fi Cation Using the Generated Ash as Oxygen Carrier Se B. *Energy Fuels* **2019**, 11552.
(13) Wilk, V.; Hofbauer, H. Co-Gasification of Plastics and Biomass in a Dual Fluidized-Bed Steam Gasifier: Possible Interactions of Fuels. *Energy Fuels* **2013**, *27*, 3261−3273.
(14) Benedikt, F.; Schmid, J. C.; Fuchs, J.; Mauerhofer, A. M.; Müller, S.; Hofbauer, H. Fuel Flexible Gasification with an Advanced 100 kW Dual Fluidized Bed Steam Gasification Pilot Plant. *Energy* **2018**, *164*, 329−343.
(15) Mattisson, T.; Keller, M.; Linderholm, C.; Moldenhauer, P.; Rydén, M.; Leion, H.; Lyngfelt, A. Chemical-Looping Technologies Using Circulating Fluidized Bed Systems: Status of Development. *Fuel Process. Technol.* **2018**, *172*, 1−12.
(16) Font Palma, C. Modelling of Tar Formation and Evolution for Biomass Gasification: A Review. *Appl. Energy* **2013**, *111*, 129−141.
(17) Abu El-Rub, Z.; Bramer, E. A.; Brem, G. Review of Catalysts for Tar Elimination in Biomass Gasification Processes. *Ind. Eng. Chem. Res.* **2004**, *43*, 6911−6919.
(18) Sutton, D.; Kelleher, B.; Ross, J. R. H. Review of Literature on Catalysts for Biomass Gasification. *Fuel Process. Technol.* **2001**, *73*, 155−173.
(19) Devi, L.; Ptasinski, K. J.; Janssen, F. J. J. A Review of the Primary Measures for Tar Elimination in Biomass Gasification Processes. *Biomass Bioenergy* **2003**, *24*, 125−140.
(20) He, H.; Boström, D.; Öhman, M. Time Dependence of Bed Particle Layer Formation in Fluidized Quartz Bed Combustion of Wood-Derived Fuels. *Energy Fuels* **2014**, *28*, 3841−3848.
(21) He, H.; Ji, X.; Boström, D.; Backman, R.; Öhman, M. Mechanism of Quartz Bed Particle Layer Formation in Fluidized Bed Combustion of Wood-Derived Fuels. *Energy Fuels* **2016**, *30*, 2227−2232.
(22) Marinkovic, J.; Seemann, M.; Schwebel, G. L.; Thunman, H. Impact of Biomass Ash−Bauxite Bed Interactions on an Indirect Biomass Gasifier. *Energy Fuels* **2016**, 4044.
(23) Kirnbauer, F.; Hofbauer, H. The Mechanism of Bed Material Coating in Dual Fluidized Bed Biomass Steam Gasification Plants and Its Impact on Plant Optimization. *Powder Technol.* **2013**, *245*, 94−104.
(24) Kuba, M.; He, H.; Kirnbauer, F.; Skoglund, N.; Boström, D.; Öhman, M.; Hofbauer, H. Mechanism of Layer Formation on Olivine Bed Particles in Industrial-Scale Dual Fluid Bed Gasification of Wood. *Energy Fuels* **2016**, *30*, 7410−7418.
(25) Marinkovic, J.; Thunman, H.; Knutsson, P.; Seemann, M. Characteristics of Olivine as a Bed Material in an Indirect Biomass Gasifier. *Chem. Eng. J.* **2015**, *279*, 555−566.
(26) Berguerand, N.; Berdugo Vilches, T. Alkali-Feldspar as a Catalyst for Biomass Gasification in a 2-MW Indirect Gasifier. *Energy Fuels* **2017**, *31*, 1583−1592.
(27) He, H.; Skoglund, N.; Öhman, M. Time-Dependent Layer Formation on K-Feldspar Bed Particles during Fluidized Bed Combustion of Woody Fuels. *Energy Fuels* **2017**, *31*, 12848−12856.
(28) Wagner, K.; Häggström, G.; Skoglund, N.; Priscak, J.; Kuba, M.; Öhman, M.; Hofbauer, H. Layer Formation Mechanism of K-Feldspar in Bubbling Fluidized Bed Combustion of Phosphorus-Lean and Phosphorus-Rich Residual Biomass. *Appl. Energy* **2019**, *248*, 545−554.
(29) Faust, R.; Hannl, T. K.; Vilches, T. B.; Kuba, M.; Öhman, M.; Seemann, M.; Knutsson, P. Layer Formation on Feldspar Bed Particles during Indirect Gasification of Wood. 1. K-Feldspar. *Energy Fuels* **2019**, *33*, 7321−7332.
(30) Hannl, T. K.; Faust, R.; Kuba, M.; Knutsson, P.; Berdugo Vilches, T.; Seemann, M.; Öhman, M. Layer Formation on Feldspar Bed Particles during Indirect Gasification of Wood. 2. Na-Feldspar. *Energy Fuels* **2019**, *33*, 7333−7346.
(31) Toftegaard, M. B.; Brix, J.; Jensen, P. A.; Glarborg, P.; Jensen, A. D. Oxy-Fuel Combustion of Solid Fuels. *Prog. Energy Combust. Sci.* **2010**, *1*, 581−625.
(32) Banaszkiewicz, T.; Chorowski, M.; Gizicki, W. Comparative Analysis of Cryogenic and PTSA Technologies for Systems of Oxygen Production. *AIP Conf. Proc.* **2014**, 1373.
(33) Fuchs, J.; Schmid, J. C.; Müller, S.; Hofbauer, H. Dual Fluidized Bed Gasification of Biomass with Selective Carbon Dioxide Removal and Limestone as Bed Material: A Review. *Renewable Sustainable Energy Rev.* **2019**, *107*, 212−231.
(34) Schweitzer, D.; Beirow, M.; Gredinger, A.; Armbrust, N.; Waizmann, G.; Dieter, H.; Scheffknecht, G. Pilot-Scale Demonstration of Oxy-SER Steam Gasification: Production of Syngas with Pre-Combustion CO2 Capture. *Energy Procedia* **2016**, *86*, 56−68.
(35) Ge, H.; Guo, W.; Shen, L.; Song, T.; Xiao, J. Biomass Gasification Using Chemical Looping in a 25 KWth Reactor with Natural Hematite as Oxygen Carrier. *Chem. Eng. J.* **2016**, *286*, 174−183.
(36) Mattisson, T.; Lyngfelt, A.; Leion, H. Chemical-Looping with Oxygen Uncoupling for Combustion of Solid Fuels. *Int. J. Greenhouse Gas Control* **2009**, *3*, 11−19.
(37) Dieringer, P.; Marx, F.; Alobaid, F.; Ströhle, J.; Epple, B. Process Control Strategies in Chemical Looping Gasification—A Novel Process for the Production of Biofuels Allowing for Net Negative CO2 Emissions. *Appl. Sci.* **2020**, *10*, No. 4271.
(38) Kramp, M.; Thon, A.; Hartge, E. U.; Heinrich, S.; Werther, J. Carbon Stripping - A Critical Process Step in Chemical Looping Combustion of Solid Fuels. *Chem. Eng. Technol.* **2012**, *35*, 497−507.
(39) Chirone, R.; Massimilla, L.; Salatino, P. Comminution of Carbons in Fluidized Bed Combustion. *Prog. Energy Combust. Sci.* **1991**, *1*, 297−326.
(40) Pissot, S.; Berdugo Vilches, T.; Thunman, H.; Seemann, M. Effect of Ash Circulation on the Performance of a Dual Fluidized Bed Gasification System. *Biomass Bioenergy* **2018**, *115*, 45−55.
(41) Bui, M.; Adjiman, C. S.; Bardow, A.; Anthony, E. J.; Boston, A.; Brown, S.; Fennell, P. S.; Fuss, S.; Galindo, A.; Hackett, L. A.; et al. Carbon Capture and Storage (CCS): The Way Forward. *Energy Environ. Sci.* **2018**, 1062.
(42) Garðarsdóttir, S. Ó.; Normann, F.; Andersson, K.; Johnsson, F. Postcombustion CO2 Capture Using Monoethanolamine and Ammonia Solvents: The Influence of CO2 Concentration on Technical Performance. *Ind. Eng. Chem. Res.* **2015**, *54*, 681−690.
(43) Lyngfelt, A.; Brink, A.; Langørgen, Ø.; Mattisson, T.; Rydén, M.; Linderholm, C. 11,000 h of Chemical-Looping Combustion Operation—Where Are We and Where Do We Want to Go? *Int. J. Greenhouse Gas Control* **2019**, *88*, 38−56.
(44) Thunman, H.; Seemann, M.; Berdugo Vilches, T.; Maric, J.; Pallares, D.; Ström, H.; Berndes, G.; Knutsson, P.; Larsson, A.; Breitholtz, C.; et al. Advanced Biofuel Production via Gasification – Lessons Learned from 200 Man-years of Research Activity with Chalmers' Research Gasifier and the GoBiGas Demonstration Plant. *Energy Sci. Eng.* **2018**, *6*, 6−34.
(45) Bruni, G.; Solimene, R.; Marzocchella, A.; Salatino, P.; Yates, J. G.; Lettieri, P.; Fiorentino, M. Self-Segregation of High-Volatile Fuel Particles during Devolatilization in a Fluidized Bed Reactor. *Powder Technol.* **2002**, *128*, 11−21.
(46) Sette, E.; Berdugo Vilches, T.; Pallarès, D.; Johnsson, F. Measuring Fuel Mixing under Industrial Fluidized-Bed Conditions – A Camera-Probe Based Fuel Tracking System. *Appl. Energy* **2016**, *163*, 304−312.

https://dx.doi.org/10.1021/acs.energyfuels.0c02781
Energy Fuels 2020, 34, 16187−16200

(47) Larsson, A.; Seemann, M.; Neves, D.; Thunman, H. Evaluation of Performance of Industrial-Scale Dual Fluidized Bed Gasifiers Using the Chalmers 2−4-MWth Gasifier. *Energy Fuels* **2013**, *27*, 6665−6680.
(48) Berdugo Vilches, T.; Seemann, M.; Thunman, H. Influence of In-Bed Catalysis by Ash-Coated Olivine on Tar Formation in Steam Gasification of Biomass. *Energy Fuels* **2018**, *32*, 9592−9604.
(49) Israelsson, M.; Seemann, M.; Thunman, H. Assessment of the Solid-Phase Adsorption Method for Sampling Biomass-Derived Tar in Industrial Environments. *Energy Fuels* **2013**, *27*, 7569−7578.
(50) Israelsson, M.; Larsson, A.; Thunman, H. Online Measurement of Elemental Yields, Oxygen Transport, Condensable Compounds, and Heating Values in Gasification Systems. *Energy Fuels* **2014**, *28*, 5892−5901.
(51) Berdugo Vilches, T.; Thunman, H. Experimental Investigation of Volatiles−Bed Contact in a 2−4 MWth Bubbling Bed Reactor of a Dual Fluidized Bed Gasifier. *Energy Fuels* **2015**, *29*, 6456−6464.
(52) Berdugo Vilches, T.; Thunman, H. In *Impact of Oxygen Transport on Char Conversion in Dual Fluidized Bed Systems*, Nordic Flame Days 2015, Copenhagen, 2015.
(53) Berdugo Vilches, T.; Marinkovic, J.; Seemann, M.; Thunman, H. Comparing Active Bed Materials in a Dual Fluidized Bed Biomass Gasifier: Olivine, Bauxite, Quartz-Sand, and Ilmenite. *Energy Fuels* **2016**, 4848.
(54) Alamia, A.; Larsson, A.; Breitholtz, C.; Thunman, H. Performance of Large-Scale Biomass Gasifiers in a Biorefinery, a State-of-the-Art Reference. *Int. J. Energy Res.* **2017**, *41*, 2001−2019.
(55) Wilk, V.; Hofbauer, H. Conversion of Mixed Plastic Wastes in a Dual Fluidized Bed Steam Gasifier. *Fuel* **2013**, *107*, 787−799.
(56) Pinto, F.; André, R.; Lopes, H.; Neves, D.; Varela, F.; Santos, J.; Miranda, M. Comparison of Co-Gasification of Wastes Mixtures Obtained from Rice Production Wastes Using Air or Oxygen. *Chem. Eng. Trans.* **2015**, 2227.

https://dx.doi.org/10.1021/acs.energyfuels.0c02781
Energy Fuels 2020, 34, 16187−16200